Reconstructing changes in nitrogen input to the Danube-influenced Black Sea Shelf during the Holocene

Andreas Neumann[1], Justus E.E van Beusekom[1], Alexander Bratek[1,2], Jana Friedrich[1,4], Jürgen Möbius[2], Tina Sanders[1], Hendrik Wolschke[3], Kirstin Dähnke[1]

1 Helmholtz-Zentrum Hereon, Institute of Carbon Cycles, Geesthacht, Germany

2 Universität Hamburg, Center for Earth System Research and Sustainability, Institute of Geology, Hamburg, Germany

3 Helmholtz-Zentrum Hereon, Institute of Coastal Environmental Chemistry, Geesthacht, Germany

4 IAEA Marine Environment Laboratories, Department of Nuclear Sciences and Applications, International Atomic Energy Agency, 98000 Monaco, Principality of Monaco

Correspondence to: Andreas Neumann (andreas.neumann@hereon.de)

Abstract. The western Black Sea shelf, where Danube River contributes the largest river discharge into the Black Sea, is particularly sensitive to river-induced eutrophication, which peaked in the 1980s and 1990s due to human-induced nutrient input. Nutrient input to the western Black Sea shelf and eutrophication is decreasing since the mid-1990s due to the collapse of eastern European economies after 1989 and ongoing mitigation measures to reduce nutrient emissions. The assessment of nutrient inputs to the Black Sea prior to the 1960s however is hindered by the scarcity of information on earlier Danube nutrient loads. Thus, to define what pristine conditions have looked like to provide a reference for nutrient reduction targets remains challenging. In this study, we aim to trace modern and historical nitrogen sources to the western Black Sea Shelf during the last ~6,000 years with special focus on the past 200 years, using sedimentary records of TOC, TIC, nitrogen, and $\delta^{15}N$.

Our results demonstrate that climate effects determine the relative contribution of riverine nitrogen and pelagic nitrogen fixation to fuel marine primary production on the NW shelf. Additionally, this balance is not only controlled by the amount of nutrients discharged by rivers, but also by the freshwater volume itself, which controls the intensity of thermohaline stratification and thereby the timing and intensity of nutrient recycling from the deep basin back into the euphotic surface water. In cold and dry sub-boreal climate pelagic N-fixation dominates over riverine N discharge, while in warm and wet Atlantic climate riverine N discharge appears as dominant N source to sustain primary production on the NW shelf. Stable nitrogen isotopes further demonstrate the increased deposition of nitrogen from human activities in all stations across the shelf and the concomitant changes in deposition rates of organic matter as indication for perturbations in the epipelagic community due to the human-induced eutrophication. Finally, our stable isotope data indicate that human-induced eutrophication can be traced back to the 11th century CE, and highlights that the Danube nutrient load was not pristine since at least 900 years.

1 Introduction

The Black Sea is a semi-enclosed sea, which is connected to the Mediterranean through the Bosphorus. The limited inflow of saline mediterranean water through the Bosporus in combination with freshwater discharge by rivers creates a strong thermohaline stratification, which separates the ventilated surface water from oxygen-free, euxinic waters, thereby creating the largest anoxic water body on earth, and hence makes the Black Sea unique. The oxycline between the ventilated surface water and the euxenic deep water promotes substantial rates of N-loss by bacterial denitrification (Fuchsman et al. 2019) or anammox (Kuypers et al. 2007) in the water column. However, H_2S in euxenic environments reduces the degradability of organic matter (Raven et al. 2018, Kok et al. 2000), which also protects the isotopic signature of nitrogen therein. Additionally, Möbius & Dähnke (2015) found that the plankton community of the Danube River Plume efficiently assimilates nitrogen from the water and thereby outcompetes ammonium oxidising and denitrifying bacteria. This means that the plankton community efficiently keeps the nitrogen in particulate organic matter until it is eventually deposited as organic matter on the shelf sediment close to the Danube Delta so that water column denitrification is not a significant sink of nitrogen on the Danube-influenced shelf.

The thermohaline stratification makes the Black Sea susceptible to climate and human pressures. The climatic oscillation in the Black Sea region between cold - dry periods and mild - wet periods appears to be governed by the North Atlantic Oscillation (NAO) and East Atlantic-West Russia (EAWR) teleconnection patterns (Oguz et al, 2006). The Black Sea exhibits a close coupling between anthropogenic and climatic forcing, as seen driving the dramatic ecosystem changes that were observed during the 1980s and 1990s (Oguz et al. 2006). The general circulation of the Black Sea is dominated by the persistent Rim Current, which circulates counterclockwise along the shelf break and horizontally mixes water masses throughout the whole basin (Oguz et al. 2005). Several coastal eddies are part of the Rim Current System and provide additional mixing across the shelf.

The north-western shelf is wider than elsewhere in the Black Sea and is substantially influenced by the discharge of several rivers (Dnipro, Dniester) of which Danube is the most significant. These rivers transport sediments into the coastal zone and the Danube built up a large Delta that spreads out into the Black Sea (Panin et al. 2016, Constantinescu et al. 2023). Additionally, Danube is the largest source of freshwater to the Black Sea, and the discharge intensity directly affects the salinity gradient in the surface water particularly in the western the Black Sea and thereby the intensity of stratification. The degree of stratification controls the vertical mixing and thus the ventilation of the deep water with oxygen and also the replenishment of N and P in the euphotic zone at the surface, which determines the susceptibility of Black Sea biogeochemical cycles to climate forcing. A high discharge of freshwater due to Atlantic climate intensifies the stratification and results in an upward shift of the oxycline and a reduced availability of nutrients in the surface water of the central Black Sea and higher availability of riverine nutrients in the river plume (Fulton et al. 2012). Conversely, low discharge of freshwater in boreal climate results in

a deep oxycline and the upwelling of deep water that is enriched in phosphorous and depleted in nitrogen (Fulton et al. 2012). Upwelling of low N and high P deep water into the surface water reduces the molar N:P ratio, which favours N-fixation (diazotrophy) and thereby reduces the proportion of riverine N in fuelling primary production (Fuchsman et al. 2008).

The Danube River is the second-largest river in Europe and hence drains a vast catchment area, which has been intensively used by humans since several millennia and thereby made this t river a significant source of nutrients to the north-western shelf. The increase in European population with spread of agricultural activities peaking first around 250 yr AD, resulted in significant deforestation in central Europe, causing erosion and hence, growth of river deltas (Maselli & Trincardi 2013, Kaplan et al. 2009). That sediment transported towards the sea led also to increased nutrient transport and hence, pre-industrial eutrophication. The recent eutrophication of Danube accelerated in the 1960 – 1990 CE period, during the 'green revolution'), which resulted in a significant eutrophication of the north-western Shelf and a degradation of habitats there (Kovacs & Zavadsky 2021). The collapse of east- European economies after 1990 CE and remediation measures later led to a substantial decrease of the Danube DIN load, which is now below the level of 1960 (Kovacs & Zavadsky 2021). Möbius and Dähnke (2015) investigated present-day nutrient inputs to the shelf and argued that the majority of riverine DIN is now taken up by primary production in the river plume and the nitrogen load being exported to the shelf in organic matter.

In this paper, we use nitrogen isotopes to identify nitrogen sources. Analysis of stable isotopes is a versatile tool as it provides distinct isotopic signatures (Kendall et al. 2007), which are expressed using the delta notation in the following. The delta notation expresses the isotopic ratio of an element in a sample (e.g. $^{15}N/^{14}N$) in relation to the isotopic ratio in a standard material, and it was designed to conveniently express the variability of isotopic ratios in natural systems in which the range is very small (McKinney et al. 1950). Nitrogen in ammonium and nitrate from fixation of atmospheric N_2 is isotopically light with $\delta^{15}N$ values around 0 ‰ (Zhang et al. 2014). This signature is preserved in organisms such as algae, which assimilate dissolved DIN to produce organic nitrogen compounds. However, molecules with the lighter ^{14}N tend to diffuse and react slightly faster than molecules with the heavier ^{15}N, which results in kinetic fractionation and slightly increases the relative concentration of ^{14}N in the product while ^{15}N is enriched in the remaining substrate. Consequently, the initial isotope signature evolves as the nitrogen is propagating though different pools. The fractionation effects of serial turnover accumulate and cause that ammonium in soils is isotopically enriched to $\delta^{15}N$ values in the range of 5 to 10 ‰, while nitrogen in manure and sewage can be isotopically enriched up to 25 ‰ (Kendall et al. 2007). Since the isotopic signature of a nitrogen pool reflects the combined effects of its history such as sources, turnover, and mixing, conclusions about the environment can be drawn from isotopic analyses. Johannsen et al. (2008) and Bratek et al. (2020) demonstrated that the $\delta^{15}N$ value of riverine nitrate is closely related to the intensity of anthropogenic land use. Dähnke et al. (2008b) and Serna et al. (2010) used the ^{15}N signature of anthropogenic nitrogen to identify the onset of human-induced eutrophication of River Elbe in sediment of North Sea and Skagerrak. Similarly, Anderson and Cabana et al. (2006) demonstrated that the $\delta^{15}N$ value of riverine nitrate is also related to the DIN load. In the following, we will apply this method to organic matter that was deposited to the sediment from the

Danube-influenced shelf to reconstruct nitrogen sources to this part of the Black Sea. Specifically, we will combine observations on N isotopes and nitrogen content to identify sources and processes. For example, if the $\delta^{15}N$ value changes but the N content remains stable, then this indicates a change in the N source. For another example, if the $\delta^{15}N$ increases and the N content decreases, then this indicates the effect of remineralisation (Möbius et al. 2013).

The present study aimed to identify present and historic nitrogen sources to the Danube-influenced north-western (NW) shelf of the Black Sea by analysing sediment cores along a transect from the Danube Delta towards the shelf break. Similar studies by Fulton et al. (2012) and Cutmore et al. (2025) focussed on sediment from the deep basins and the continental slope of the Black Sea but did not cover the north-western shelf where the major rivers discharge into the Black Sea. Aiming to close this gap, our samples along a transect from the Danube Delta towards the shelf break reflect the gradient from a dominant influence of the Danube River Plume to the dominant influence of water masses from the open Black Sea, which both imprint the specific signature of their respective nitrogen sources into the sediment record. We analysed the sediment for organic carbon and nitrogen, and the composition of stable nitrogen isotopes to identify natural and anthropogenic nitrogen sources over the past 7,000 years.

2 Material & Methods,

2.1 Working area and samples

Sampling was performed in early May 2016 during R/V Mare Nigrum cruise MN 148 in the Romanian Shelf area at four stations that span a transect from nearshore to offshore (Tab. 1, Fig. 1). The water depth at the sampling stations ranged from 22 m (Station 2) to 80 m (Station 6). From each station, sediment cores (20-40 cm length, 6 cm in diameter) were taken with a Multicorer. The sediment cores were immediately sliced in 1 cm intervals and frozen for further analysis. The sediment from stations 4 and 6 was wet sieved through a 400 µm sieve after slicing to collect mussel shells for radiocarbon dating. The <400 µm fraction was freeze-dried and homogenized for analysis of $\delta^{15}N$, organic carbon and nitrogen content.

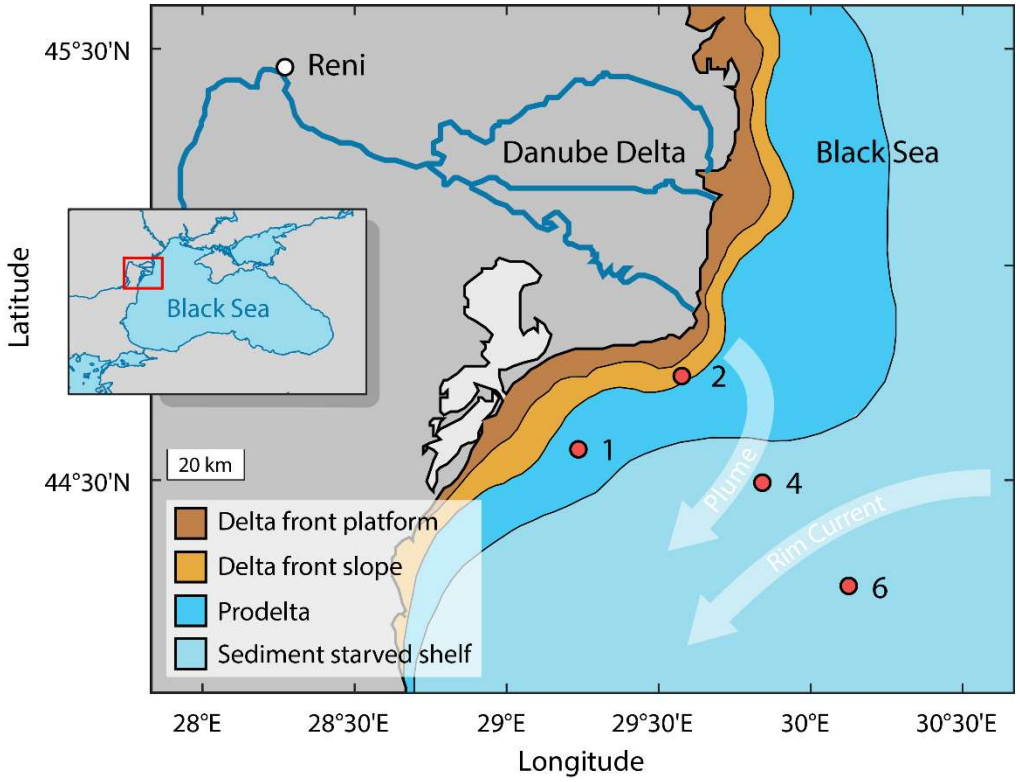

Figure 1: Map showing the sampling stations of the sediment cores 1, 2, 4 and 6 in the northwestern Black Sea during RV Mare Nigrum cruise 148 and major depositional units of the Danube Delta (after Panin et al. 2016). The light arrows indicate the general surface water currents of Danube River Plume and Rim Current. The insert map indicates the study area (red rectangle) within the Black Sea area.

Table 1: Summary of meta data of sediment cores from Mare Nigrum cruise 148.

Core	Latitude	Longitude	Water depth (m)	Core length (cm)
1	45° 58.4	29° 18.8‘	30	42
2	44° 74.9	29° 58.2‘	22	35
4	44° 49.9	29° 84.8‘	62	29
6	44° 25.2	30° 13.1‘	80	27

2.2 Analyses of sediment samples

The sediment samples were analysed for total carbon and total nitrogen content with an elemental analyser (Carlo Erba NA 1500) via gas chromatography, calibrated against acetanilide. The total organic carbon content (TOC) was analysed after a threefold removal of inorganic carbon using 1 mol L^{-1} hydrochloric acid. Sediment carbonate content was then calculated as the difference of total carbon content and TOC content. The standard deviation of sediment samples was less than 0.6% for TOC and 0.08 % for nitrogen.

Nitrogen isotope analyses were performed with a CE 1108 elemental analyser (Thermofinnigan) connected to a mass spectrometer (Finnigan 252) via a split interface (Conflow). Two international standards were used for calibration (IAEA-N1: $\delta^{15}N = 0.4$ ‰, IAEA-N2: $\delta^{15}N = 20.3$ ‰), and an additional, internal standard was measured for further quality assurance. The standard deviation for repeated measurements was < 0.2 ‰.

2.3 Radiocarbon Dating

The radiocarbon ages of organic sediment (TOC) were obtained from 2 bulk sediment samples from Station 4, and 6 bulk sediment samples from Station 6. Additionally, 6 bivalve shells from different sediment layers of Station 6 (two samples of *Modiolula phaseolina* and four samples of *Mytilus galloprovincialis*) were analysed to date the carbonate. These two species were used because the top 8 cm of the sediment are characterized by *Modiolula phaseolina*, whereas *Mytilus galloprovincialis* is dominant in deeper layers. The radiocarbon analyses were carried out at Beta Analytic Inc., U.K., following standard procedures for accelerator mass spectrometry (AMS) radiocarbon dating. The radiocarbon ages are corrected for $\delta^{13}C$. Radiocarbon ages were calibrated to years before present (0 a BP_{1950} = 1950 CE) using the Marine20 calibration curve (Heaton et al. 2020). The sample ages were further corrected with a reservoir age of -111 ± 63 years (N = 5), based on data from Romanian and Bulgarian shelf sediment as provided by the Marine Reservoir Correction Database (Reimer & Reimer 2001). The age of sediment samples between dated samples was estimated by linear interpolation.

2.4 ^{210}Pb, ^{137}Cs Dating

For ^{137}Cs, ^{226}Ra, and ^{210}Pb measurement low-level gamma spectrometry was used. Sample preparation was carried out as described in Bunzel et al. (2020). Briefly, the cores were sectioned into slices of 1 cm thickness and frozen during transportation and storage. Each section was dried and homogenized by a ball mill. Aliquots of each sample were sealed in gas-tight Petri dishes and stored for minimum 28 days for equilibration of Radium-226 with daughter isotopes ^{222}Rn, ^{214}Pb and ^{214}Bi. Measurements were performed by a high-purity low-level germanium detector (BE 3830P-7500SL-ULB Mirion Technologies / Canberra, Ruesselsheim, Germany). Measurement times varied between 90 000 s - 600 000 s depending on sample activity. For calibration an artificial reference material was prepared from silica gel and reference solutions of ^{137}Cs and ^{226}Ra. (Eckert & Ziegler Nuclitec GmbH, Braunschweig, Germany). Sediment ages were calculated from ^{210}Pb results according to the CRS

model (Appleby & Oldfield 1978), assuming a constant rate of supply of atmospheric ^{210}Pb. For consistent use of units, all ^{210}Pb dating results are stated in years before present with 1950 CE as 0 (in a BP_{1950}).

2.5 Data integration and analyses

Sediment ages of cores 1 and 2 are based on results of Constantinescu et al. (2023), which sampled the same stations simultaneously and applied ^{210}Pb and ^{137}Cs dating. Observed Danube DIN loads are based on data from Kovacs & Zavadsky (2021), which presented DIN loads at Reni station at the upstream margin of the Danube Delta (Fig. 1). Both datasets were mapped to the corresponding sediment depths of cores 1 and 2 by linear interpolation. As the result, an interpolated ^{210}Pb / ^{137}Cs age and an interpolated DIN load was assigned to each of our sediment measurements of cores 1 and 2.

Using the interpolated DIN load and measured sediment N concentration, we derived two linear models from the DIN load – sediment N content correlation: Model 1 without y- intercept and Model 2 with y intercept. From the DIN load – δ^{15}N correlation, we derived Model 3.

The apparent isotopic fractionation factor (ε) was calculated by means of Rayleigh plots (Möbius 2013). From the analysed subset of sediment samples, we used the largest value of the total N content as the reference for the calculation of the remaining fraction (f), which consequently plots at the coordinate origin.

Based on δ^{15}N vs. N content plots we visually identified sediment layers with similar conditions. The underlying assumption was that in periods with a roughly constant trend in δ^{15}N vs. N content indicates that a particular condition dominated during this period.

2.6 Data transformation

The age data in Figure 7 were log transformed to emphasise the results from the most recent centuries. The data include age values after 1950 CE, which have a negative sign on the BP_{1950} scale and can't be log transformed. All plotted age data were thus converted to the BP_{2020} scale where 0 a BP_{2020} refers to the year 2020 CE. The axis labels correspond to the BP_{1950} scale, so that when reading data from the diagram, the age data is displayed in the BP_{1950} scale.

3 Results

3.1 Radioisotope measurements and dating

Sediment organic matter at Station 4 was dated 1035 ± 97 a BP at 7.5 cm core depth and 2837 ± 98 a BP at 16.5 cm core depth by radiocarbon (^{14}C) dating. The age of organic sediment at Station 6 spans from 137 ± 93 a BP at the sediment surface to 5679 ± 104 a BP at 16.5 cm depth. Radiocarbon-based ages of bivalve shell carbonates at Station 6 span from 3504 ± 108 a BP at the sediment surface to 5880 ± 110 a BP at 16.5 cm depth. The results of radiocarbon dating are summarised in Table 2 and plotted in Figure 2. At Station 6, dated carbonates were systematically older than the organic sediment, and this difference was larger at the sediment surface than at depths (Tab. 2, Fig. 2). Ultimately, organic sediment and carbonate shells represent two different carbon pools, which are affected individually by early diagenesis. In the following, we will focus only on the organic sediment. No radiocarbon measurements were performed on sediment of Station 1 and 2.

Additional to ^{14}C, we measured ^{137}Cs and unsupported ^{210}Pb in Station 4 sediment, where unsupported ^{210}Pb was highest at the sediment surface (306 Bq / kg dry sed.) and decreased exponentially with depth. ^{210}Pb was below detection limit below 4 cm sediment depth (Fig. 2). The estimated sediment ages ranged from -75 a BP at 0.5 cm sediment depth to 44 a BP at 3.5 cm sediment depth. Similarly, ^{137}Cs activity was highest at the sediment subsurface (79 Bq / kg dry sed.), but was detectable to deeper sediment layers than unsupported ^{210}Pb (Fig. 2). No ^{210}Pb and ^{137}Cs measurements of sediment from Station 6 are available.

Table 2: Results of radiocarbon dating of organic sediment and carbonate shells from Cores 4 and 6, and calibrated age ± 1 sd, using Marine20 and ΔR = -111 ± 63 a. 0 a BP equals 1950 CE.

Core	Sediment depth (cm)	Material	Conventional ^{14}C age (a)	Calibrated age (a BP)
4	7.5	organic sediment	1530 ± 30	1035 ± 97
4	16.5	organic sediment	3080 ± 30	2837 ± 98
6	0.5	organic sediment	560 ± 30	137 ± 93
6	4.5	organic sediment	2180 ± 30	1727 ± 109
6	7.5	organic sediment	3550 ± 30	3408 ± 108
6	11.5	organic sediment	4280 ± 30	4348 ± 121
6	16.5	organic sediment	4790 ± 30	5004 ± 126
6	19.5	organic sediment	5380 ± 30	5679 ± 104
6	0.5	carbonate (*Modiolula phaseolina*)	3630 ± 30	3504 ± 108
6	7.5	carbonate (*Modiolula phaseolina*)	3490 ± 30	3334 ± 105
6	7.5	carbonate (*Mytilus galloprovincialis*)	4380 ± 30	4484 ± 123
6	11.5	carbonate (*Mytilus galloprovincialis*)	4650 ± 30	4823 ± 121
6	16.5	carbonate (*Mytilus galloprovincialis*)	5380 ± 30	5679 ± 104
6	19.5	carbonate (*Mytilus galloprovincialis*)	5570 ± 30	5880 ± 110

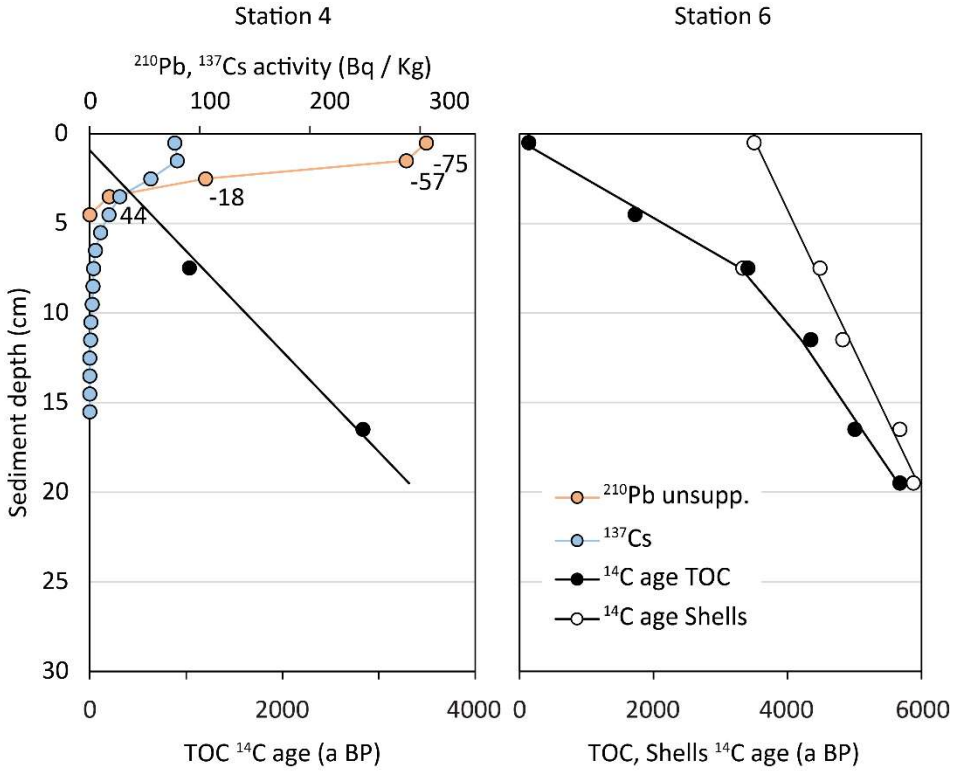

Figure 2: Results of radioisotope analyses of Cores 4 and 6: Radiocarbon (^{14}C) ages of organic sediment (black circles), radiocarbon ages of carbonate shells (white circles). Measurements of unsupported ^{210}Pb (orange circles) and ^{137}Cs (blue circles). Numbers along ^{210}Pb plot indicate sediment age according to CRS model. No ^{210}Pb or ^{137}Cs data are available for Core 6.

3.2 Sediment cores

The characteristics of sampled sediment reflected the proximity of the respective stations to the shore and the Danube Delta. Station 1 was in the shallow Prodelta (Fig. 1), where the sediment was layered mud with various shades of grey, and black layers at 28 cm, 37 cm, 41 cm, and 44 cm sediment depth. Living *Mytilus* bivalves were found at the top layer and empty *Mytilus* shells within the black layers. Core 2 was sampled from the delta front slope (Fig. 1), and sediment was layered mud with various shades of beige, grey, and black. The sediment record of core 2 is affected by the sharp increase of sand content in some layers, which are the result of increased transport of sand from the Sfantu George branch due to the cutting off all the meanders in Sfantu Gheorghe between 1984 and 1988, which led to an accelerated flow, riverbed erosion and transport of coarser sediment in the main channel of that branch. Stations 4 and 6 are located on the sediment staved shelf (Fig. 1) where

sedimentation rates are lowest. In Core 4, the top 0-3.5 cm were *Modiolula* shells in grey mud, then grey mud without shells down to 6 cm, and light grey mud from 6 to 26 cm sediment depth. Similarly in Core 6, *Modiolula* shells in mud were found at the top 0-5 cm, followed by light grey mud in 5-10 cm, and grey mud in 10-15 cm sediment depth. In 15-20 cm sediment depth, we found dark grey mud, and black mud with *Mytilus* shells in 20-25 cm depth.

3.3 Bulk sediment characteristics

Generally, N stable isotopic composition of sediment ($\delta^{15}N$) follows a gradient from the shore towards to open Black Sea: The entire nearshore sediment cores of stations 1 and 2 are isotopically enriched (mean $\delta^{15}N$ = 6.7 ‰) with respect to atmospheric N_2 ($\delta^{15}N$ = 0.0 ‰), while the distant stations were isotopically less enriched and were as light as 1.6 ‰. The nearshore sediment cores had lower concentration in organic matter than the more offshore cores.

Sediment from stations 1 and 2 was distinct from stations 4 and 6. While sediment close to the delta at stations 1 and 2 consisted of silt, silty clay and very fine sand, the sediment starved shelf station 4 and 6 sediment consisted of shelly clay (*Modiolula* and *Mytilus*). In detail, sediment at station 1 had contents of TOC (1.2 – 2.9 % d.w.), TIC (1.1 – 2.1 % d.w.), and N (0.12 – 0.30 % d.w.). While TOC and N had a maximum in 17 cm sediment depth, TIC had no discernible variation with sediment depth. The molar TOC / N ratio decreased from 15 at the sediment surface to 8 at 18 cm sediment depth and increased again to 10 at 35 cm. Sediment at station 2 was similarly low in TOC, TIC, and N content had only small variation with sediment depth. TOC contents were in the range of 0.7 to 1.9 % dry weight, the TIC contents in the range of 1.3 to 1.8 % dry weight, and N contents in the range of 0.05 to 0.26 % dry weight. The molar TOC / N ratio increased significantly from 8 at 35 cm sediment depth to 15 at the sediment surface, while no significant variation in $\delta^{15}N$ values was observed (Fig. 3). The stations 4 and 6 on the continental slope were markedly different from stations 1 and 2. At station 6, small shell fragments of the bivalve *Modiolula phaseolina* were present in the upper 8 cm. Below 8 cm depth, bivalve shells of *Mytilus galloprovinialis* were found. At these stations, the organic carbon and nitrogen content decreases in the upper 3 to 7 cm of the cores (TOC 1.1 to 4.0 %; N 0.10 to 0.42 %, Fig. 3). At station 4, there is a slight increase in organic carbon (1.0 to 2.5 %) and nitrogen (0.10 to 0.30 %) content below 7 cm depth. The TOC and TN contents strongly increased with depth at station 6 (TOC: 2.7 to 9.2 %, N: 0.3 to 1.0 %). In contrast, the molar TOC / N ratios decreased with sediment depth at station 4 and slightly increased with depth at station 6 (Fig. 3 K, L).

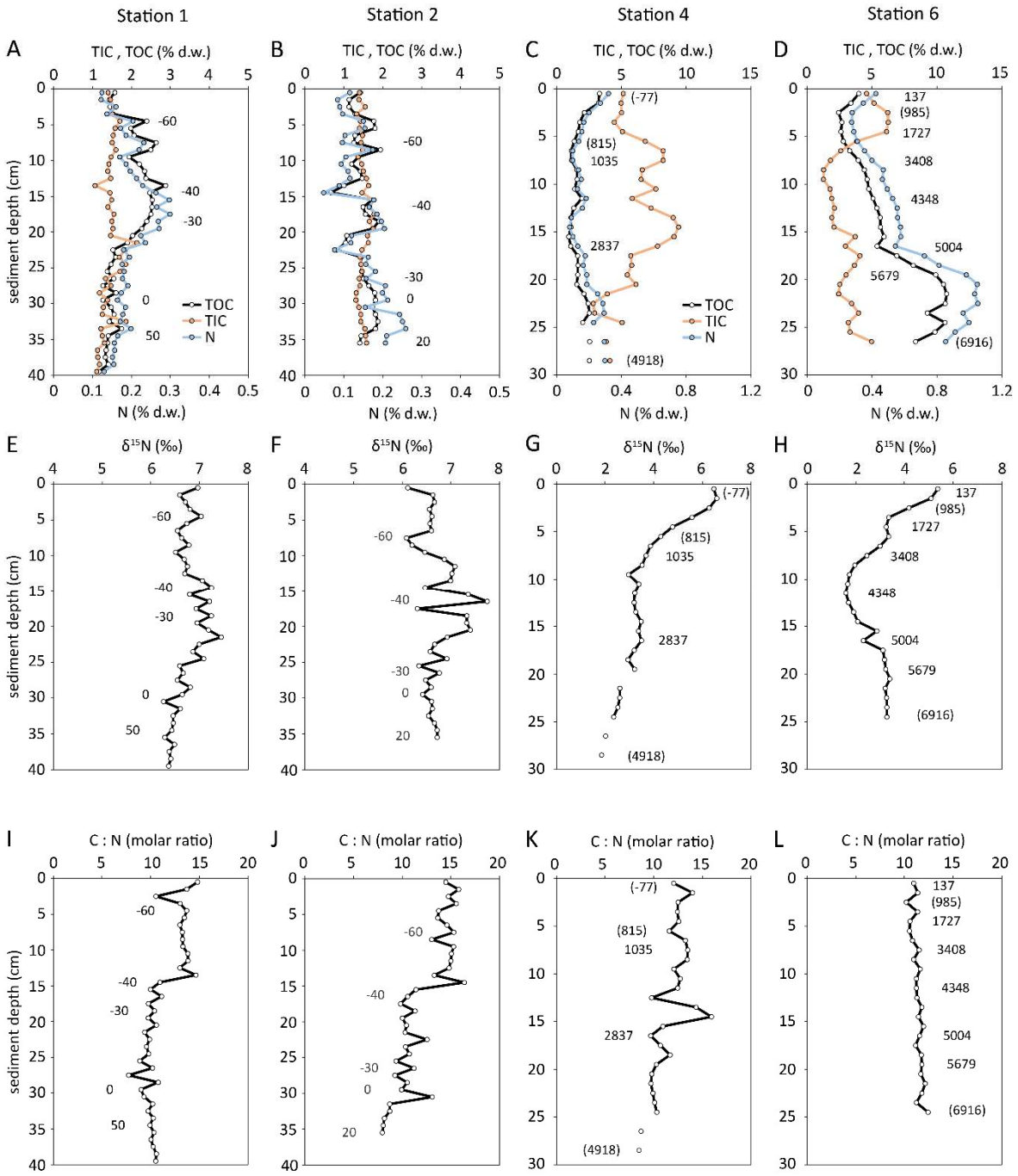

255 **Figure 3: From Stations 1- 6, depth profiles of TIC (carbonate), TOC (organic sediment), total nitrogen (panels A - D), measured $\delta^{15}N$ values of bulk sediment (panels E – H), and molar TOC / N ratio of organic sediment (panels I – L). Numbers refer to the sediment age BP (0 a BP = 1950 CE, negative age values are after 1950 CE, positive age values are before 1950 CE), based on ^{210}Pb (Stations 1, 2) and ^{14}C (Stations 4, 6). Numbers in parentheses were estimated by linear interpolation. ^{210}Pb data from Constantinescu et al. (2023).**

3.4 N isotope signatures

Based on the $\delta^{15}N$ vs. N content plots of Figure 4, we identified 4 zones with distinct trends in N content and $\delta^{15}N$ value. At the sediment surface, N content increased towards the sediment surface and N isotopes were most enriched (Fig. 4, filled circles), and we reference this sediment layer as Zone 1 in the following. Zone 1 comprised the whole sampled sediment column at the coastal stations 1 and 2, and sediment in this layer had $\delta^{15}N$ values in the range 6 – 7 ‰ and N content around 0.2 % (Fig. 4 A, B). In the deeper stations 4 and 6, $\delta^{15}N$ values were in the range 4 – 6.5 ‰ and N content roughly around 0.3 % (Fig. 4 C, D). Zone 1 reaches back until ca. 900 a BP (Fig. 4 C, D). Below the sediment layer of Zone 1, the trend of $\delta^{15}N$ vs. N content changes clearly. The $\delta^{15}N$ values still increased towards the surface, but the N content decreased, and we refer to this sediment layer as Zone 2. The $\delta^{15}N$ values increased from ca. 2 ‰ to ca. 4 towards the surface, while the N content decreased from ca. 0.4 % to 0.2 % (open circles in Fig. 4 C, D). Since the trend of $\delta^{15}N$ vs. N content in the sediment layer indicates kinetic fractionation by remineralisation, data from this layer were further analysed for the apparent isotope enrichment factor (ε) by means of Rayleigh plots. The estimated values were $\varepsilon = -1.1 \pm 0.2$ ‰ for Station 4, and $\varepsilon = 3.0 \pm 0.3$ ‰ for Station 6, respectively (Fig. 5). In Core 4, this Zone went back to 4.9 ka BP, and in Core 6 back to 4.3 ka BP.

The Zones 3 and 4 were only present at station 6. Sediment in the layer of Zone 3 was characterized by a constant N content of ca. 0.6 % while $\delta^{15}N$ values were decreasing from ca. 3 ‰ down to 1.6 ‰ (Fig. 4 D, closed triangles). This layer was dated 5.0 ka BP to 4.3 ka BP. Zone 4 is characterised by N contents that decreased from ca. 1.1 % down to 0.6 %, while $\delta^{15}N$ values were constant at ca. 3.3 ‰ (Fig. 4, open triangles). Zone 4 comprised sediment from the bottom end of the core with an age of 6.9 ka BP to sediment with an age of 5.0 ka BP.

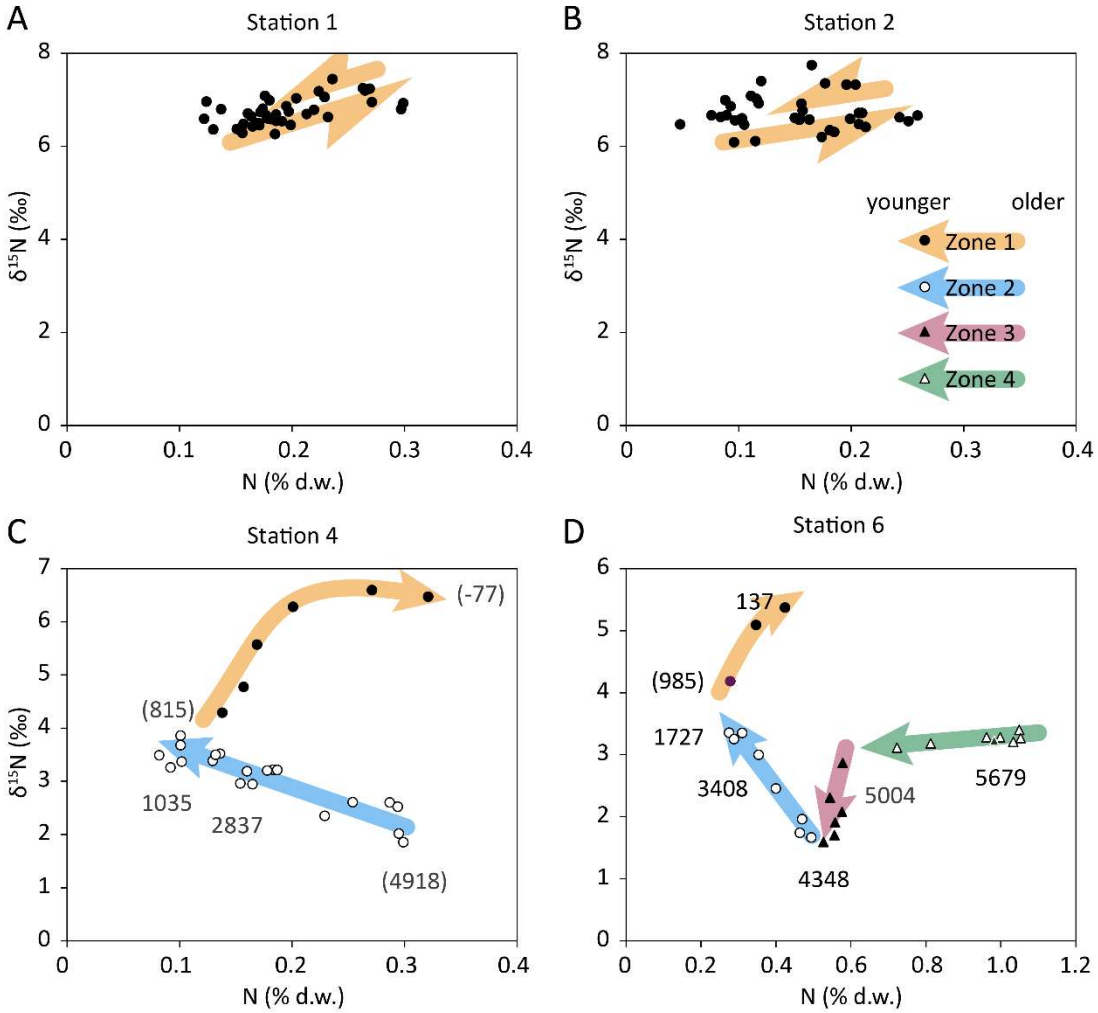

Figure 4: Sedimentary $\delta^{15}N$ vs. sedimentary nitrogen concentrations at Station 1 (A), Station 2 (B), Station 4 (C), and Station 6 (D). The different symbols indicate different process zones within the sediment column: Zone 1) filled circles indicate modern eutrophication, Zone 2) open circles indicate diagenetic enrichment, Zone 3) filled triangles indicate the gradual transition between two isotopically distinct nitrogen sources, and Zone 4) open triangles indicate Unit II sapropel. Numbers refer to the ^{14}C-based sediment age, numbers in parentheses were estimated by linear interpolation. Coloured arrows represent the arrow of time for distinct trends of $\delta^{15}N$ vs. N content.

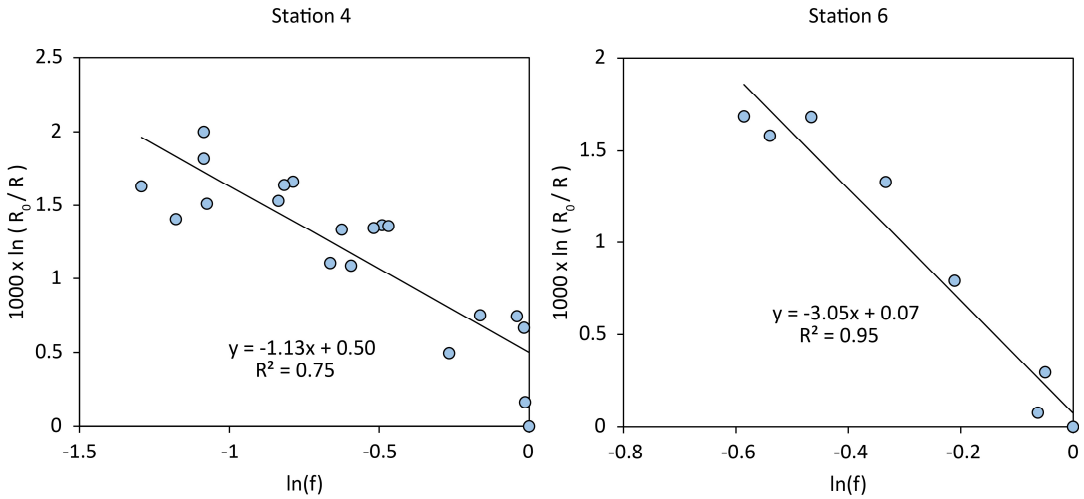

Figure 5: Rayleigh plots of $\delta^{15}N$ vs. sedimentary N content of samples from Zone 2 of Stations 4 and 6 (see also Figure 4 C, D, open circles).

295

3.5 Danube DIN load models

The correlation of Danube DIN loads with sediment N contents and $\delta^{15}N$ values in the nearshore cores 1 and 2 at a given time was examined to develop a simple empirical model for reconstructing historical DIN loads for the period before measurements are available. Using core 2, no meaningful correlation was found (not shown). Using core 1, the DIN load of Danube at Reni
300 station (Kovacs & Zavadsky 2021) correlated significantly with the bulk N content (Pearson's R = 0.80) and less significant with $\delta^{15}N$ (Pearson's R = 0.35, Model 3). The N content-based Models 1 and 2 had average residuals with respect to observed DIN loads of 36 ± 26 kt / yr and 42 ± 31 kt / yr, respectively (Fig. 6 B, D). The average residuals of the $\delta^{15}N$-based Model 3 were 61 ± 33 kt / yr (Fig. 6 F). For the period 1800 – 1950, all three models estimated that the Danube DIN load was 236 to 318 kt / yr in 1800 CE and increased gradually with 0.2 to 0.5 kt / yr^2.

305

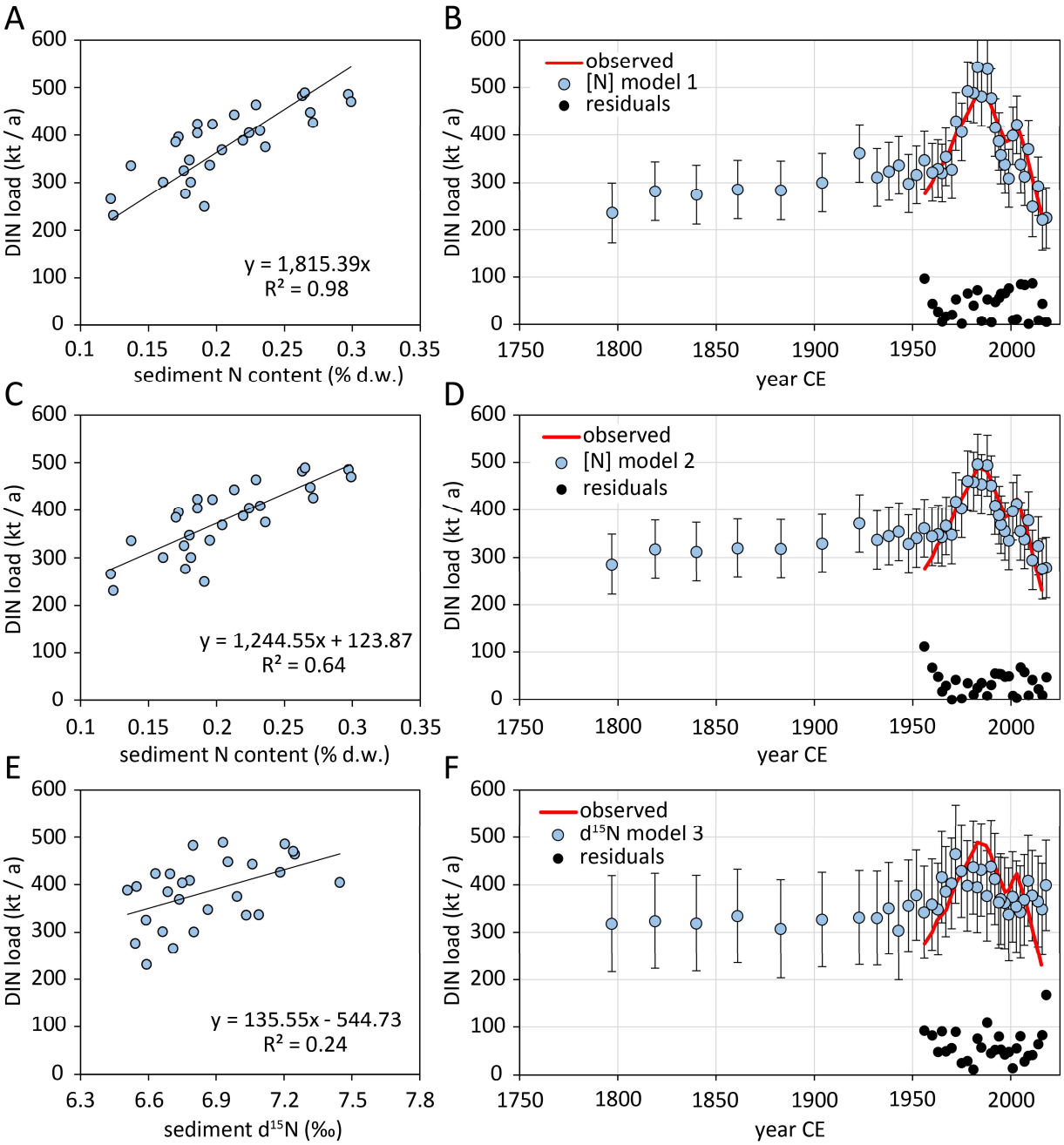

Figure 6: Linear correlations of Danube DIN loads with sediment N content at station 1 at a given time, based on sediment dating (Constantinescu et al, 2023) (A, C) and sediment $\delta^{15}N$ values (E), and reconstructed DIN loads based on these correlations (B, D, F). Error bars indicate prediction intervals with 90 % confidence. Red lines indicate DIN observation data for 1955 – 2015, data from Kovacs & Zavadsky (2021).

4 Discussion

4.1 Overview

Based on $\delta^{15}N$ and N content measurements on sediment from the NW shelf we identified four distinct sediment layers where each one is characterised by a distinct combination of $\delta^{15}N$ and N content dynamics (Fig. 4), and we thus assume that these four layers represent the record of distinct conditions on the NW shelf. In the following, we will interpret the data from these four Zones and discuss the implications for the major nitrogen sources for the primary productivity on the shelf during these periods

We start by combining data from cores 1, 4, and 6 into a joint plot to construct a composite timeline plot (Fig. 7) and to read the sediment record imprinted in the northwestern shelf. We excluded data from Core 2 due to the absence of correlation of Danube DIN load and sedimentary N content and $\delta^{15}N$ (see results, 3.3). The individual $\delta^{15}N$ plots are matching well in periods where the plots are overlapping and the continuity of the composed $\delta^{15}N$ plot suggests that organic matter in the water column was mixed across the entire shelf prior to deposition on the sediment (Fig. 7). Similarly, we combined the N content data from cores 1, 4, and 6, and found systematic offsets between the cores (Fig. 7) in the sense that sediment farther from the delta had higher N content than sediment from the same period that was deposited closer to the delta. However, we still find simultaneous variations of N content over time, which we interpret as a result of higher deposition rates of terrigenous material closer to the delta. The corresponding sedimentation rates of terrigenous matter were up to 10 mm yr^{-1} close to the delta (Constantinescu et al. 2023) and as low as 0.03 mm yr^{-1} (Tab. 2) at the deeper shelf. The higher sedimentation rates closer to the delta effectively diluted the deposited organic matter more than the low sedimentation rates did farther from the delta.

Now we continue to discuss our observations from the four distinct $\delta^{15}N$ / N Zones (Fig. 4) individually to elucidate how variations in climate forcing, stratification of the water column, and human activity are reflected in the sediment record of the NW shelf.

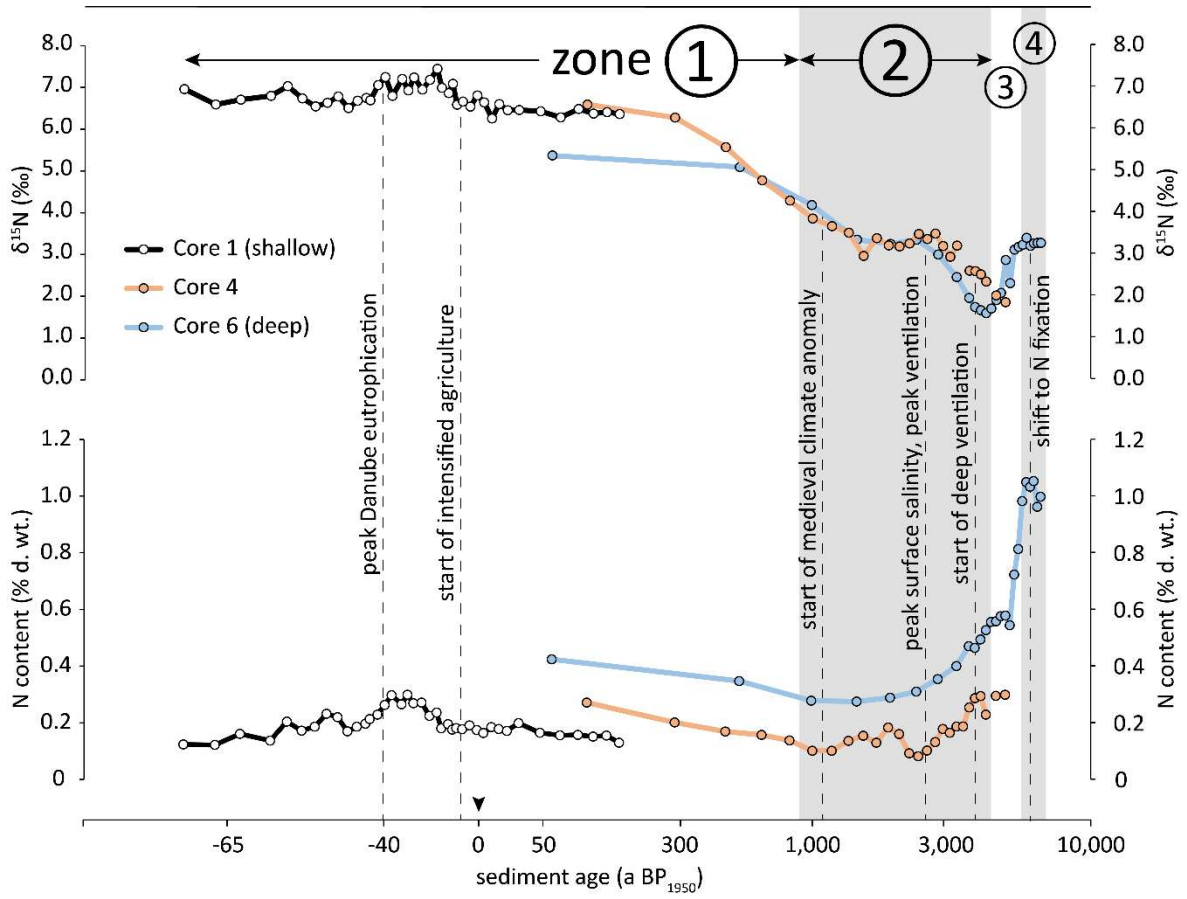

Figure 7: Evolution of N content and $\delta^{15}N$ values in sediment cores 1, 4 and 6 from the NW shelf, Grey and white backgrounds indicate $\delta^{15}N$ / [N] zones 1 – 4, additionally marked by circled numbers. Vertical dashed lines mark significant events mentioned in the following discussion. Age scale is log transformed (see methods 2.6 for details).

4.2 Strong stratification and sapropel formation: 6.9 - 5.7 ka BP

The oldest sediment we found in our cores dates back 6.9 ka BP at station 6. At that time, the Black Sea was influenced by a humid Atlantic climate with high freshwater input from the rivers and seawater influx from the Mediterranean through the Bosphorus, leading to a strong thermohaline stratification and a shallow chemocline. The shallow chemocline at that time was confirmed by Cutmore et al. (2025) through the presence of isorenieratene in the sediment, which is an indicator of the chemocline being so shallow that hydrogen sulphide ascended into the photic zone. These euxinic conditions would have substantially constrained the degradation of sinking particles in the water column and in the sediment once they have been deposited. As a result, measured isotopic values of sediment from this period are probably close to the original isotopic

signature. We indeed measured a $\delta^{15}N$ value of 3.3 ‰ in this sediment layer, which is consistent with riverine N from a pristine catchment with no anthropogenic land use (Johannsen et al. 2008, Bratek et al. 2020) and thus indicates that riverine nitrogen was the dominant N source to the NW shelf. Fulton et al. (2012) reconstructed the $\delta^{15}N$ value of phytoplankton in the range of 1.4 to 4.4 ‰ for this period, and our results agree with this reconstruction. We thus conclude that the N / $\delta^{15}N$ trend of Zone 4 (Fig. 4 open triangles, Fig. 7) indicates the sapropel with high organic matter concentration that was deposited in the Black Sea basins during this phase and was termed stratigraphic unit II b (Ross et al. 1970). Our data from this period had similarly high TOC values in Core 6 and a matching $\delta^{15}N$ value of 3.3 ‰ (Fig. 3).

4.3 Shift to Nitrogen Fixation: 5.0 - 4.4 ka BP

The humid Atlantic phase lasted until approx. 5.1 ka BP and was replaced by sub-boreal climate, which was colder and dryer. The sub-boreal climate resulted in substantially reduced riverine input and a weakened salinity gradient due to increased surface salinity (Giosan et al. 2012). The weaker stratification led to a deeper circulation, which enhanced the pelagic ventilation (Fulton et al. 2012). We observed a clear change in bulk $\delta^{15}N$ values and N content around 5.0 ka BP at the most offshore station 6 and found a similarly low $\delta^{15}N$ value of 1.9 ‰ in station 4 sediment (Fig. 3, open circles) from the period in which deep circulation may have favoured N-fixation (Fig. 7, Zone 3). We suggest that the N source gradually shifted from riverine N to N-fixation in the 5.0 – 4.4 ka BP period and is represented by the N / $\delta^{15}N$ trend of Zone 3 (Fig. 4 closed triangles, Fig. 7). The sediment of this period is equivalent with sediment Unit II a, which is the upper part of the organic-rich sapropel layer (Ross et al. 1970). The intensified and deeper mixing of the water column would not only mix oxygen downwards but would also enable the upward transport of nitrogen depleted and phosphate enriched deep water into the surface water, which resulted in N : P ratios in the euphotic zone in the range of 3.5 – 6 and which thereby favoured N- fixation by cyanobacteria (Fulton et al. 2012). The reconstructed $\delta^{15}N$ value of phytoplankton during this period was in the range of 0.3 to 2.1 ‰ (Fulton et al. 2012), which in combination with additional proxies confirms dominant N-fixation (Cutmore et al. 2025). N-fixation has a strong negative isotopic effect and results in plankton with a comparatively low $\delta^{15}N$ value in the range of approximately -2 to 1 ‰ (Minagawa & Wada 1986). However, the $\delta^{15}N$ values we have observed in sediment from the NW shelf are slightly higher than the values observed by Fulton et al. (2012) and Cutmore et al. (2025), which have sampled locations farther from the Danube Delta and with deeper bottom depth. This offset hints that isotopically heavier N from riverine inputs had a higher contribution to the N supply at the NW shelf than at more distant parts of the Black Sea.

4.4 Oxygenated sediment at the shelf break: 4.4 - 0.9 ka BP

The intensified and deeper circulation during the sub-boreal phase resulted in an intensified ventilation of the shelf water as confirmed by Cutmore et al. (2025), which did not detect the proxy for H_2S in the photic zone during this period (3.9 – 2.7 ka BP) while this proxy (isorenieratene) was always present before and after this period and thereby indicates an exceptional deep

ventilation. The deeper ventilation of the water column gradually increased the exposure of shelf sediments to oxygen and thereby enabled enhanced remineralisation of deposited organic matter there. Möbius et al. (2010) demonstrated that early diagenesis is indicated by increasing $\delta^{15}N$ values and decreasing N concentrations, which we indeed found in Cores 4 and 6 in the period 4.4 to 0.9 ka BP (marked as Zone 2 in in Fig. 4, Fig. 7). During this period, the highest $\delta^{15}N$ value and lowest N concentration coincided with the peak of surface water salinity (Giosan et al. 2012), which we interpret as an indication that benthic remineralisation was most pronounced when the salinity gradient was weakest and thus ventilation was most intense (Fig. 7).

In Core 4, the apparent enrichment factor of $\varepsilon = -1.1 \pm 0.2$ ‰ falls well within the range of published values for remineralisation of organic matter (Möbius et al. 2010), and we think that the observed increase in $\delta^{15}N$ values in Zone 2 is rather a result of remineralisation and not an indication of changes in nitrogen sources. However, we found a different situation in Core 6, where the apparent enrichment factor of the same period was much higher ($\varepsilon = -3.0 \pm 0.3$ ‰) and would be unusual for remineralisation alone. We thus assume that Core 6 reflects the combined effect of early diagenesis and a gradual shift from N fixation to isotopically more enriched riverine N input.

In summary, we conclude that between 4.4 – 0.9 ka BP station 4 was supplied by a more or less stable mixture of N from river discharge and from pelagic nitrogen fixation. The more offshore station 6 was initially supplied by isotopically depleted nitrogen from N-fixation circa 4.4 ka BP, which was gradually complemented by isotopically enriched nitrogen until 0.9 ka BP (Fig. 4). This would imply that the influence of the Danube River plume extended from station 4 to station 6 in this period. At around 1.0 ka BP, $\delta^{15}N$ values of sediment from Cores 4 and 6 were around 4 ‰, which is substantially above the values reported by Fulton et al. (2012) and Cutmore et al. (2025) for this period, which reported $\delta^{15}N$ values of 1 ‰ and 0.5 ‰, respectively. This difference underlines that the sediment record from the NW shelf reflects different processes than the sediment from more distant parts of the Black Sea.

Into the period 4.4 – 0.9 ka BP also falls the occurrence of coccoliths from the haptophyte plankton algae *Gephyrocapsa huxleyi* (formerly *Emiliania huxleyi*) in the sediment, which starts approximately at 3.6 ka BP (Hay et al. 1991, Coolen 2011). We find a corresponding increase in TIC in sediment from Cores 4 and 6 from 3.6 ka BP onwards until approx. 0.9 ka BP (Fig. 3). Since low water N:P ratios not only favour N-fixation but also enable *G. huxleyi* to form blooms (Lessard et al. 2005), the presence of coccoliths might indicate that the outer shelf was still influenced by N-deficit and thus by N-fixation.

4.5 Anthropogenic eutrophication and recovery: 900 a BP to present

At around 900 a BP_{1950}, we observed an increase in $\delta^{15}N$ values and N content, which indicates that the condition changed on the NW shelf. The $\delta^{15}N$ values eventually exceeded the values from Zone 1 when N from pristine rivers was the dominant N

source. Instead, the high $\delta^{15}N$ values indicate the deposition of N that was isotopically enriched by human activities (Johannsen et al. 2008, Bratek et al. 2020). The deposition of substantially enriched N apparently started around 900 ± 120 a BP_{1950} in cores 4 and 6 (Figure 7), and thus much earlier than the industrialisation in the 20th century when the usage of artificial fertiliser became widespread. Fulton et al. (2012) and Cutmore et al. (2025) consistently found a significant increase of sediment $\delta^{15}N$ values in cores from the shelf and deep basins, starting at around 0.5 ka BP_{1950}, which supports our observation that the deposition of enriched nitrogen began much earlier than the industrialisation. The difference of approximately 400 years between the onset of enriched nitrogen deposition on the Danube influenced shelf (this study) and the deeper locations further south (Fulton et al. 2012, Cutmore et al. 2025) most likely reflects the differences in the sensitivity of these locations to signals from the Danube.

The apparently early onset of isotopically enriched nitrogen deposition could be an artifact of bioturbation in which benthic macrofauna mixes modern, isotopically enriched nitrogen from the sediment surface downwards and thus into older sediment layers. The sediment cores retrieved at stations 4 and 6 were populated by sessile tunicates and small bivalves (*Modiolula phaseolina*), which are not strong bioturbators and are unlikely to provide sufficient sediment mixing to transport anthropogenic ^{15}N down to 7 cm sediment depth at station 4. Our measurements of particle-associated ^{210}Pb further indicates that the mixed surface layer reaches down to 4 cm at maximum (Fig. 2), which is significantly above the deepest occurrence of enriched nitrogen at 7 cm depth (Fig. 3). The deeper penetration of ^{137}Cs does not contradict our interpretation as ^{137}Cs has a higher mobility in marine sediment as ^{210}Pb and has probably migrated into deeper sediment layers as described by Wang et al. 2022. Additionally, the carbonate content of Cores 4 and 6 decreased simultaneously with increased $\delta^{15}N$, which is not a plausible result of sediment mixing by bioturbation. Instead, the decreasing carbonate content in the modern surface layer indicates a change in the nutrient regime with a shift from coccolithophorid blooms to dinoflagellate blooms in the coastal area (Giosan et al. 2012).

An explanation for the early deposition of enriched nitrogen likely could be the intensified N discharge during the Medieval Warm Period / Medieval Climate Anomaly (Mann et al. 2009). During this local climate optimum in Europe between 1000 and 700 a BP_{1950}, a substantial population growth led to expansion of agricultural land use and urbanization and thereby to substantial deforestation in Europe (Giosan et al. 2012). The Medieval Climate Anomaly coincides with the onset of anthropogenic N deposition on the NW shelf (Fig. 7). The pre-industrial eutrophication of the Danube River is further supported by our reconstruction of Danube DIN loads for the 19th century (Fig. 6). The modelled DIN loads based on correlations of observed DIN load and sedimentary bulk nitrogen content suggest that the Danube DIN load was in the range of 236 to 286 kt / a in 1800 CE, which is in the range of the current load (Kovacs & Zavadsky 2021). Although the river DIN load with shelf sediment $\delta^{15}N$ values were substantially less correlated than with shelf sediment bulk N content, the reconstructed DIN load based on $\delta^{15}N$ is similar to the N content-based results. Additionally, the average slope of the Danube River DIN load trend in 1800 – 1950 of 0.35 ± 0.16 kt / yr^2 can be linearly extrapolated approximately 800 years backwards

until the modelled Danube River DIN load approaches zero. Although this extrapolation reaches very far into the past with respect to the relatively short period of underlying observation data and is thus an estimate with a substantial amount of uncertainty, our model results are in line with an early onset of anthropogenic eutrophication of Danube. Our approach to reconstruct historical Danube River DIN loads relies on the assumption that quantity and isotopic composition of Danube River DIN translate linearly to Black Sea sedimentary N content or bulk $\delta^{15}N$ values, although the dissolved N is assimilated into phytoplankton, transported, deposited in the delta, and partially degraded by early diagenesis. The approach appears valid for the 1955 – 2015 period, and we are not aware of conflicting results to challenge our approximations of historic Danube DIN loads. The results of the offshore stations 4 and 6, which go far back into the past, in combination with results from the coastal station 1, which recorded the N deposition of the last 200 years in more detail, give a coherent picture of the steadily increasing eutrophication of the Danube for at least 900 ± 120 years, which has only decreased again in the last 30 years. The sediment record of Station 2 is not reflecting these processes in sufficient detail likely due to its location on the active delta front slope (Fig. 1). The sediment there is biased by sand deposits from the Sfanthu George Danube branch as a results of cutting off all the meanders of Sfantu Gheorghe, between 1984 and 1988, which led to an accelerated flow in the main channel and scouring of its river bed (Constantinescu et al, 2023).

The youngest major event reflected in the sediment record is the massive eutrophication during the 'Green Revolution' starting in the 1960s with intensified discharge of nutrients, resulting in enhanced primary production, enhanced oxygen consumption due to enhanced organic matter decomposition in deeper water layers, and thus a shallower oxycline. The increased deposition of organic matter with isotopically enriched nitrogen is evident in all cores and is especially obvious in core 1. There, the highest N content and highest $\delta^{15}N$ values coincided with the peak of eutrophication during the 1980- 1990 period (-30 to -40 a BP_{1950}, see Fig. 3, Fig. 7) and decreased simultaneously when the nitrogen load of Danube significantly dropped after the 1990s (Kovacs & Zavadsky 2021).

If our hypothesis is true that the eutrophication of Danube started several centuries before the onset of industrialisation, this would further imply that Danube was not pristine in the sense of the European Water Frame Directive (WFD) since the Middle Ages. The WFD requests from EU member states to manage water bodies at the river basin level to achieve "good status" for all water bodies, which basically requests a condition with no or minimal human impact (European Commission, 2000), including the riverine nutrient load. The outcome of our study indicates that defining good status of a water body based on zero or minimal human impact may not be possible for some systems as such conditions are difficult to reconstruct. In contrast, it may be recommended to base good environmental status on the ecosystem functions of the water body and those ecosystems associated to it.

Conclusions

We have sampled sediment across the NW shelf of the Black Sea along a gradient from high influence of Danube close to the Danube Delta to low influence close to the shelf break. We analysed the nitrogen stable isotope composition and the nitrogen content of the sediment to identify nitrogen sources to the primary production on the NW shelf. Our results indicate that the relative contribution of riverine nitrogen and pelagic N-fixation fluctuated during the past 7,000 years and was largely driven by climate changes. Due to the proximity of our sampling sites to the Danube Delta, which made the sediment record there more susceptible to signals from the Danube, we found that the deposition of isotopically enriched nitrogen started approximately 900 years ago. We attribute the isotopically enriched nitrogen to human activities, and the deposition of substantial amounts of nitrogen from anthropogenic activities started surprisingly long before the industrialisation, which is commonly believed to have induced the current eutrophication in the 20th century. Instead, Danube was not pristine with respect to nutrient loads since the Middle Ages. Our reconstructed DIN loads suggest that Danube was already eutrophicated at 1800 CE at a similar level as present, and that DIN loads gradually increased throughout the 19th and 20th century until 1960 CE. Then, eutrophication steeply increased even further and peaked around 1990 CE due to intensified agriculture, the so-called Green Revolution. After 1990, The Danube River DIN loads decreased significantly due to economic collapse in the early 1990s and nutrient reduction policies afterwards in the Danube River catchment, and this reduction of the Danube N-load is already reflected in the western Black Sea coastal sediment record.

Author contributions

Conceptualization: AN, AB, JEEvB, JF, JM, TS, KD; Formal analysis: AN, AB, JM, HW; Investigation: JEEvB, AB, JM, HW Visualization: AN, Writing (original draft preparation): AN, Writing (review and editing): AN, JEEvB, JF, JM, TS, HW, KD.

Competing interests

The authors declare that they have no conflict of interest.

Financial support

This study was supported by the project ReCoReD (Reconstructing the Changing Impact of the Danube on the Black Sea and Coastal Region) funded by TNA FP7 EuroFleets 2, and by the DOORS project (European Commission, Grant 101000518).

Acknowledgement

We wish to thank the captain and the crew of the RV *Mare Nigrum*. We are grateful to M. Ankele, M. Metzke and N. Lahajnar for analytical work. We further thank L. Hoffman for the taxonomic identification of bivalve shells. The International Atomic Energy Agency is grateful to the Government of the Principality of Monaco for the support provided to its IAEA Marine

Environment Laboratories. We appreciate the comments of three anonymous reviewers to further improve our manuscript. No so-called AI tools have been used for this study.

References

Anderson C., Cabana G.: Does delta15N in river food webs reflect the intensity and origin of N loads from the watershed? Sci Total Environ. 2006 Aug 31;367(2-3):968-78. doi: 10.1016/j.scitotenv.2006.01.029, 2006.

Appleby P. G., Oldfield, F.: The Calculation of Lead-210 Dates Assuming a Constant Rate of Supply of Unsupported ^{210}Pb to the Sediment. Catena, 5, 1-8. DOI: 10.1016/S0341-8162(78)80002-2. 1978

Bratek A., Emeis K.-C., Sanders T., Wankel S. D., Struck U., Möbius J., Dähnke K.: Nitrate sources and the effect of land cover on the isotopic composition of nitrate in the catchment of the Rhône River, Isotopes in Environmental and Health Studies, 56:1, 14-35, DOI: 10.1080/10256016.2020.1723580, 2020.

Bunzel D., Milker, Y., Müller-Navarra, K., Arz, H.W., Friedrich, J., Lahajnar, N., Schmiedl, G.: Integrated stratigraphy of foreland salt-marsh sediments of the south-eastern North Sea region. Newsletters Stratigr. 53, 415–442. https://doi.org/10.1127/nos/2020/0540, 2020.

Constantinescu A. M., Tyler A. N., Stanica A., Spyrakos E., Hunter P. D., Catianis I., Panin N.: A century of human interventions on sediment flux variations in the Danube-Black Sea transition zone. Front. Mar. Sci. 10:1068065. doi: 10.3389/fmars.2023.1068065, 2023.

Coolen M. J. L.: 7000 Years of *Emiliania huxleyi* Viruses in the Black Sea. Science, 333(6041), 451–452. doi:10.1126/science.1200072, 2011.

Cutmore A., Bale N., Hennekam R., Yang B., Rush D., Reichart G.-J., Hopmans E. C., Schouten S.: Impact of deoxygenation and hydrological changes on the Black Sea nitrogen cycle during the Last Deglaciation and Holocene, Clim. Past, 21, 957–971, https://doi.org/10.5194/cp-21-957-2025, 2025.

Dähnke K., Serna A., Blanz T., Emeis K.-C.: Sub-recent nitrogen-isotope trends in sediments from Skagerrak (North Sea) and Kattegat: Changes in N-budgets and N-sources? Marine Geology 253: 92-98. DOI: 10.1016/j.margeo.2008.04.017, 2008.

European Commission, 2000: Directive 2000/60/EC of the European Parliament and of the Council of 23 October 2000 establishing a framework for community action in the field of water policy. Off. J. Eur. Communities, 2000.

Fuchsman C. A., Murray J. W., Konovalov, S. K.: Concentration and natural stable isotope profiles of nitrogen species in the Black Sea. Marine Chemistry, 111(1), 90-105. DOI: 10.1016/j.marchem.2008.04.009, 2008.

Fuchsman C. A., Paul B., Staley J. T., Yakushev E. V., Murray J. W.: Detection of transient denitrification during a high organic matter event in the Black Sea. Global Biogeochemical Cycles, 33, 143–162, DOI: 10.1029/2018GB006032, 2019.

Fulton J. M., Arthur M. A., Freeman K. H.: Black Sea nitrogen cycling and the preservation of phytoplankton δ^{15}N signals during the Holocene, Global Biogeochem. Cycles, 26, GB2030, DOI:10.1029/2011GB004196, 2012.

Giosan L., Coolen M., Kaplan J. *et al.*: Early Anthropogenic Transformation of the Danube-Black Sea System. Sci Rep 2, 582, DOI: 10.1038/srep00582, 2012.

Hay B. J., Arthur M. A., Dean W. E., Neff E. D., Honjo S.: Sediment deposition in the Late Holocene abyssal Black Sea with climatic and chronological implications. Deep Sea Research Part A. Oceanographic Research Papers, 38, S1211–S1235. doi:10.1016/S0198-0149(10)80031-7, 1991.

Heaton T. J., Köhler P., Butzin M., Bard E., Reimer R.W., Austin W.E.N., Bronk Ramsey C., Hughen K.A., Kromer B., Reimer P.J., Adkins J., Burke A., Cook M.S., Olsen J., Skinner L.C.: Marine20-the marine radiocarbon age calibration curve (0-55,000 cal BP). Radiocarbon 62. DOI: 10.1017/RDC.2020.68. 2020.

Johannsen A., Dähnke K., Emeis K.-C.: Isotopic composition of nitrate in five German rivers discharging into the North Sea, Organic Geochemistry 39(12), 0–1689. DOI: 10.1016/j.orggeochem.2008.03.004, 2008.

Kaplan J. O., Krumhardt K. M., Zimmermann N. The prehistoric and preindustrial deforestation of Europe. Quaternary Science Reviews 28, 3016–3034, DOI: 10.1016/j.quascirev.2009.09.028, 2009.

Kendall C., Elliott E. M., Wankel S. D.: Tracing anthropogenic inputs of nitrogen to ecosystems, Stable isotopes in ecology and environmental science, 2, 375-449, 2007.

Kok M. D., Schouten S., Sinninghe Damsté J. S.: Formation of insoluble, nonhydrolyzable, sulfur-rich macromolecules via incorporation of inorganic sulfur species into algal carbohydrates. Geochim. Cosmochim. Acta 64, 2689–2699, 2000.

Kovacs A., Zavadsky, I.: Success and sustainability of nutrient pollution reduction in the Danube River Basin: recovery and future protection of the Black Sea Northwest shelf. Water International, 46(2), 176–194. DOI: 10.1080/02508060.2021.1891703, 2021.

Kuypers M., Sliekers A., Lavik G. et al.; Anaerobic ammonium oxidation by anammox bacteria in the Black Sea. Nature 422, 608–611, DOI: 10.1038/nature01472, 2003.

Lessard E., Merico A., Tyrrell T.: Nitrate: Phosphate Ratios and Emiliania huxleyi Blooms. Limnology and Oceanography. 50. 1020-1024. DOI: 10.4319/lo.2005.50.3.1020, 2005.

Mann M. E. *et al.*: Global Signatures and Dynamical Origins of the Little Ice Age and Medieval Climate Anomaly. Science 326,1256-1260, DOI:10.1126/science.1177303, 2009.

McKinney C.R., McCrea J.M., Epstein S., Allen H.A., Urey H.C.: Improvements in mass spectrometers for the measurement of small differences in isotope abundance ratios. Rev Sci Instrum 21:724–730, 1950.

Maselli V., Trincardi F.: Man made deltas. Scientific Reports 3, 1926, DOI: 10.1038/srep01926, 2013.

Minagawa M., Wada E.: Nitrogen Isotope Ratios of Red Tide Organisms in the East-China-Sea – a Characterization of Biological Nitrogen-Fixation, Mar. Chem., 19, 245–259, DOI: 10.1016/0304-4203(86)90026-5, 1986.

Möbius J., Lahajnar N., Emeis, K.-C.: Diagenetic control of nitrogen isotope ratios in Holocene sapropels and recent sediments from the Eastern Mediterranean Sea, Biogeosciences, 7, 3901–3914, DOI: 10.5194/bg-7-3901-2010, 2010.

Moebius, J.: Isotope fractionation during nitrogen remineralization (ammonification): Implications for nitrogen isotope biogeochemistry. Geochimica et Cosmochimica Acta. 422-432. DOI:10.1016/j.gca.2012.11.048, 2013.

Möbius J., Dähnke K.: Nitrate drawdown and its unexpected isotope effect in the Danube estuarine transition zone. Limnology and Oceanography 60: 1008-1019, DOI: 10.1002/lno.10068, 2015.

Oguz T., Tuğrul S., Kideys A., Ediger V., Kubilay N.: Physical and biogeochemical characteristics of the Black Sea. The Sea. 14. 1331-1369, 2005.

615 Oguz, T., Dippner, J. W., Kaymaz, Z.: Climatic regulation of the Black Sea hydro-meteorological and ecological properties at interannual-to-decadal time scales. Journal of Marine Systems, 60(3-4), 235-254, DOI: 10.1016/j.jmarsys.2005.11.011, 2006.

Panin N., Duţu L. T., Duţu F.: The Danube Delta, Méditerranée, 126, 37-54. DOI: 10.4000/mediterranee.8186, 2016.

620 Raven M. R., Fike D. A., Gomes M. L., Webb S. M., Bradley A. S., McClelland H.-L. O.: Organic carbon burial during OAE2 driven by changes in the locus of organic matter sulfurization. Nat. Commun. 9, 3409, 2018.

Reimer P.J., Reimer R.W.: A marine reservoir correction database and on-line interface. Radiocarbon 43:461-3, 2001.

625 Ross D. A. et al.: Black Sea: Recent Sedimentary History, Science 170, 163-165, DOI:10.1126/science.170.3954.163, 1970.

Serna A., Pätsch J., Dähnke K., Wiesner M. G., Hass H. C., Zeiler M., Hebbeln D., Emeis K.-C.: History of anthropogenic nitrogen input to the German Bight/SE North Sea as reflected by nitrogen isotopes in surface sediments, sediment cores and hindcast models. Continental Shelf Research 30: 1626-1638, DOI: 10.1016/j.csr.2010.06.010, 2010.

630

Wang J.L., Baskaran M., Cukrov N., Du J.: Geochemical mobility of ^{137}Cs in marine environments based on laboratory and field studies, Chemical Geology, 614, Article 121179, DOI: 10.1016/j.chemgeo.2022.121179, 2022.

Zhang X., Sigman D. M., Morel F. M. M., Kraepiel, A. M. L.: Nitrogen isotope fractionation by alternative nitrogenases and
635 past ocean anoxia, Proceedings of the National Academy of Sciences, 111, 4782-4787, doi:10.1073/pnas.1402976111, 2014.